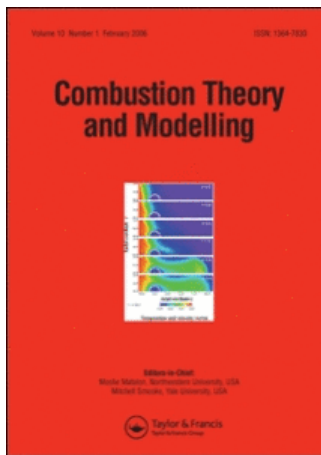


This article was downloaded by:[Cornell University]  
On: 21 May 2008  
Access Details: [subscription number 789515533]  
Publisher: Taylor & Francis  
Informa Ltd Registered in England and Wales Registered Number: 1072954  
Registered office: Mortimer House, 37-41 Mortimer Street, London W1T 3JH, UK



## Combustion Theory and Modelling

Publication details, including instructions for authors and subscription information:

<http://www.informaworld.com/smpp/title~content=t713665226>

### Time-averaging strategies in the finite-volume/particle hybrid algorithm for the joint PDF equation of turbulent reactive flows

Haifeng Wang<sup>a</sup>; Stephen B. Pope<sup>a</sup>

<sup>a</sup> Sibley School of Mechanical and Aerospace Engineering, Cornell University, Ithaca, NY, USA

First Published: June 2008

To cite this Article: Wang, Haifeng and Pope, Stephen B. (2008) 'Time-averaging strategies in the finite-volume/particle hybrid algorithm for the joint PDF equation of turbulent reactive flows', *Combustion Theory and Modelling*, 12:3, 529 — 544

To link to this article: DOI: 10.1080/13647830701847875

URL: <http://dx.doi.org/10.1080/13647830701847875>

PLEASE SCROLL DOWN FOR ARTICLE

Full terms and conditions of use: <http://www.informaworld.com/terms-and-conditions-of-access.pdf>

This article maybe used for research, teaching and private study purposes. Any substantial or systematic reproduction, re-distribution, re-selling, loan or sub-licensing, systematic supply or distribution in any form to anyone is expressly forbidden.

The publisher does not give any warranty express or implied or make any representation that the contents will be complete or accurate or up to date. The accuracy of any instructions, formulae and drug doses should be independently verified with primary sources. The publisher shall not be liable for any loss, actions, claims, proceedings, demand or costs or damages whatsoever or howsoever caused arising directly or indirectly in connection with or arising out of the use of this material.

## Time-averaging strategies in the finite-volume/particle hybrid algorithm for the joint PDF equation of turbulent reactive flows

Haifeng Wang\* and Stephen B. Pope

*Sibley School of Mechanical and Aerospace Engineering,  
Cornell University, Ithaca, NY 14853, USA*

*(Received 16 May 2007; final version received 30 November 2007)*

The influence of time-averaging on bias is investigated in the finite-volume/particle hybrid algorithm for the joint PDF equation for statistically-stationary turbulent reactive flows. It is found that the time-averaging of the mean fluctuating velocity (TAU) leads to the same variances of the fluctuating velocity before and after the velocity correction, whereas without TAU the estimates are different, and an additional numerical dissipation rate is introduced for the turbulent kinetic energy (TKE). When 100 particles per cell are used without TAU, a large bias error is found to be involved in the unconditional statistics of the statistically-stationary solutions of two tested turbulent flames, the Cabra  $H_2/N_2$  lifted flame and the Sandia piloted flame E. The use of TAU reduces this bias dramatically for the same number of particles per cell. The conditional statistics in these flames, however, are hardly affected by TAU. To a large extent, the effect of the bias error on the unconditional statistics is similar to the effect of increasing the model constant  $C_{\omega 1}$  in the stochastic turbulence frequency model.

**Keywords:** bias; numerical dissipation; numerical method; PDF method; time-averaging

### 1. Introduction

The probability density function (PDF) method [1, 2] has achieved considerable success in the numerical simulation of turbulent combustion problems. Some complicated turbulent combustion phenomena (e.g., local extinction and re-ignition) can be predicted quantitatively [3–7]. The success of the PDF method benefits from the parallel development of physical models and numerical methods. The physical models include the PDF transport equation and the corresponding stochastic differential equations (SDEs) [1, 2], models for the Lagrangian velocity, turbulence frequency [8] and acceleration [9], and mixing models [10]. Numerical methods include the Monte Carlo particle method [1, 11, 12], and the hybrid finite-volume (FV)/particle method [13–16]. It is very important to ensure and demonstrate the numerical accuracy of computed results, so as to eliminate numerical error as a possible source of discrepancies between model calculations and experimental measurements. In this work, the numerical accuracy of the PDF calculations is further tested and related to previous work [5, 6, 15, 17].

The PDF calculations considered here are performed by using a code called HYB2D which implements the consistent hybrid finite-volume (FV)/particle solution algorithm for the joint PDF transport equation [15]. During the development of the PDF solution algorithms, from the stand-alone particle/mesh method (implemented in the code PDF2DV) [3, 18] to the current hybrid

---

\*Corresponding author. Email: hw98@cornell.edu

method [15], the numerical error has been carefully evaluated [12, 15, 18]. Compared to the stand-alone particle/mesh method, the hybrid method reduces the bias dramatically [15]. In order to understand better the bias error reduction in the hybrid method, the influence of the time-averaging technique on the bias is re-investigated. Time-averaging is a powerful technique to reduce the statistical error [18] and to some extent the bias [14, 15]. We show here that the time-averaging of the mean fluctuating velocity can reduce the bias dramatically. In the hybrid method [15], the fluctuating velocity is a property of each particle. Due to statistical error, the mass-weighted mean of the fluctuating velocity from particles is not zero, and a velocity correction is performed for the fluctuating velocity of each particle by subtracting an estimate of the mean fluctuating velocity. Mean quantities such as the mean fluctuating velocity, which are estimated from the particles and fed back into the particle solver, are referred to as particle-to-particle quantities.

One motivation for the current work is to investigate the impact of time-averaging on calculations of the Sandia piloted flames, since time-averaging of particle-to-particle quantities was not used in some previously reported calculations [5, 6]. Various test cases indicate that only the time-averaging of the mean fluctuating velocity in the particle-to-particle quantities reduces the bias significantly, and the time averaging of the other particle-to-particle quantities has a negligible effect on the final solution. Hence only the influence of the time-averaging of the mean fluctuating velocity on the bias is discussed in this work.

In the following section, the hybrid algorithm in HYB2D is briefly summarized, the time-averaging strategies are described, and then the bias due to the velocity correction is analysed. In Section 3, the effect of time-averaging on the bias involved in the unconditional and condition statistics is evaluated for two test cases, the Cabra  $H_2/N_2$  lifted flame [19] and the Sandia piloted flame E [20]. The choice of the value of the model constant  $C_{\omega_1}$  and its interaction with numerical error are discussed in Section 4. Conclusions are drawn in the final section.

## 2. Time-averaging in HYB2D

### 2.1. Summary of HYB2D

The hybrid method (implemented in the code HYB2D) [15] solves the transport equation for the joint PDF of velocity, turbulence frequency and composition for turbulent combustion problems. The finite volume (FV) method is used to solve the mean conservation equations for mass, momentum, and energy and the mean equation of state; and the particle method is used to solve the transport equation of the joint PDF of the fluctuating velocity, turbulence frequency and composition. The FV part provides the mean fields of velocity, density and pressure to the particle part and obtains all the Reynolds stresses, the turbulent fluxes and the mean chemical source term from the particle part. The hybrid method is consistent at the level of the governing partial differential equations. At the numerical level, the consistency conditions are identified, and the correction algorithms are devised in [15], where the details of the hybrid solution algorithm can be found.

### 2.2. Time-averaging technique

HYB2D is applicable to statistically-stationary flows by using a pseudo-time marching method. The PDF is represented by an ensemble of particles. Starting from some initially specified properties, the method marches the particles in time steps  $\Delta t$  to approach the statistically-stationary solution. At a given time step, the mean fields are estimated from the particles. A statistical error which varies as  $N_{pc}^{-1/2}$  [1] (where  $N_{pc}$  is the number of particles per cell) is involved in the estimate of mean fields. After the statistically-stationary state is reached, this error

can be reduced by time-averaging [18]. For a quantity used solely for output, time-averaging reduces statistical error, but not bias. Part of the origin of bias is from statistical fluctuations in quantities fed back into the calculations. Hence the use of time-averaging to reduce these fluctuations reduces the bias. Following [15], the time-averaging scheme is defined, for a mean field  $Q$ , as

$$Q_{TA}^j = \left(1 - \frac{1}{N_{TA}^j}\right) Q_{TA}^{j-1} + \frac{1}{N_{TA}^j} Q^j, \quad (1)$$

where  $Q_{TA}^j$  and  $Q^j$  are the time-averaged and instantaneous values evaluated on the  $j$ th time step, and  $N_{TA}^j$  is a time-averaging parameter to be specified, which is abbreviated to  $N_{TA}$  when it is not necessary to explicitly show the dependence on  $j$ . Note that  $N_{TA}^j = 1$  corresponds to no time-averaging, and in general we have  $N_{TA}^j \geq 1$ .

Two different types of quantities in HYB2D are time-averaged: first, output quantities for postprocessing such as conditional or unconditional means and rms of temperature, species mass fractions; and, second, quantities which are fed back into the calculations, such as turbulent fluxes, and the mean chemical source term.

For output quantities, the time-averaging strategy used is called the uniform-time-averaging (UTA). UTA is turned on after the statistically-stationary state has been reached (indicated here as the time step  $j_0$ ). By turning on UTA, the time-averaged quantities for the output at the  $j$ th time step ( $j > j_0$ ) become

$$\begin{aligned} Q_{TA}^j &= \frac{1}{j - j_0 + 1} \sum_{i=j_0}^j Q^i \\ &= \left(1 - \frac{1}{j - j_0 + 1}\right) \frac{1}{j - j_0} \sum_{i=j_0}^{j-1} Q^i + \frac{1}{j - j_0 + 1} Q^j \\ &= \left(1 - \frac{1}{j - j_0 + 1}\right) Q_{TA}^{j-1} + \frac{1}{j - j_0 + 1} Q^j. \end{aligned} \quad (2)$$

It may be seen that Equation (2) corresponds to the general definition of time-averaging (Equation (1)) with  $N_{TA}^j$  specified as  $N_{TA}^j = j - j_0 + 1$ . The statistical error involved in the time-averaged output quantities scales as  $(N_{pc} N_{TA}^j)^{-1/2}$  for  $\Delta t N_{TA}^j$  large compared to the correlation time of the statistical error [13, 18], so the statistical error of the output can be reduced by using UTA for many time steps and for a fixed number of particles per cell  $N_{pc}$ . Usually, for a typical run, more than 5000 steps ( $N_{TA}^j > 5000$ ) are time-averaged uniformly to reduce the statistical error. The UTA of the output quantities, however, cannot reduce the bias involved in the solution which scales as  $N_{pc}^{-1}$  [12, 18].

Time-averaging of the feedback quantities is able to reduce the bias because of the reduced statistical fluctuations in these quantities. In the hybrid algorithm, there are three categories of feedback fields to be time-averaged [17]. The first category is the mean quantities from particles fed back into the evolution of particles (referred as particle-to-particle quantities, e.g., mean fluctuating velocity and turbulence frequency). The second category consists of the particle mean fields passed to the FV solver (e.g., Reynolds stresses, turbulent fluxes). The last category consists of the FV fields. A different strategy called moving-time-averaging (MTA) is used for these feedback quantities. The time-averaging scheme (Equation 1) is used with a different

specification of the parameter  $N_{TA}^j$ . Initially, all the time-averaging strategies (MTA and UTA with  $N_{TA}^j = 1$ ) are disabled to make the transient process most rapid. After a certain number of time steps, a statistically-stationary state is reached, which is determined by monitoring the time series of particle ensemble mean quantities. This statistically-stationary state involves bias. By using MTA, the statistical error and the bias are reduced gradually, so the previous statistically-stationary state changes on a time scale of  $T_{TA} = N_{TA} \Delta t$  and a different statistically-stationary state is approached. In order to reduce the statistical error and bias,  $N_{TA}^j$  is increased gradually, but it is limited to a specified maximum  $N_{max}$ , i.e.,  $N_{TA}^j = \min[1 + 0.25 \times \max(j - j_0, 0), N_{max}]$  where  $j_0$  is the time step from which MTA is used. This upper limit  $N_{max}$  is imposed so that the time scale  $T_{TA}$  is not too large to allow the time-averaged quantities to follow any residual transients. On time step  $j$  ( $j > j_0$ ), the time-averaged quantity  $Q_{TA}^j$  is

$$\begin{aligned} Q_{TA}^j &= \left(1 - \frac{1}{N_{TA}^j}\right) Q_{TA}^{j-1} + \frac{1}{N_{TA}^j} Q^j \\ &= \sum_{i=j_0}^j \frac{1}{N_{TA}^i} \left[ \prod_{k=i+1}^j \left(1 - \frac{1}{N_{TA}^k}\right) \right] Q^i, \end{aligned} \quad (3)$$

so the contribution of  $Q^i$  to  $Q_{TA}^j$  is weighted by  $\frac{1}{N_{TA}^i} [\prod_{k=i+1}^j (1 - \frac{1}{N_{TA}^k})]$ . In HYB2D, the value of  $N_{max}$  is different for different categories of feedback quantities, i.e., the value of  $N_{max} = 500$  [17, 23] is used for the particle-to-particle quantities, and  $N_{max} = 5$  [17] is used for the particle-to-FV quantities and for the FV fields. In previous work [17, 23], these values were deemed to provide satisfactory performance, but they may not be optimal.

The procedure of using the time-averaging in HYB2D during the time marching is the following. Initially, all the time-averaging strategies are turned off to make the transient process most rapid. After the statistically-stationary state is approximately reached, MTA is turned on to reduce the statistical error and the bias of the stationary solution. With more than 5000 steps of MTA, a statistically-stationary solution with less bias is obtained. Then, UTA of the output quantities is turned on to further reduce the statistical error involved in these quantities. With another 5000 steps of UTA, the output quantities are sufficiently time-averaged and are ready for the postprocessing: then the run terminates.

### 2.3. Bias due to the velocity correction

The condition of zero mean density-weighted fluctuating velocity ( $\langle \rho \mathbf{u} \rangle / \langle \rho \rangle = 0$ , where angle brackets denote mathematical expectation) is identified as one of the three independent consistency conditions in the hybrid algorithm [15]. The fluctuating velocity is a property of a particle in the current PDF algorithm. The mass weighted ensemble mean of the particle fluctuating velocity  $\tilde{\mathbf{u}}$  pertaining to a FV cell, on a particular time step, is defined as

$$\tilde{\mathbf{u}} = \frac{\sum_{k=1}^N \mathbf{u}^{(k)} m^{(k)}}{\sum_{k=1}^N m^{(k)}}, \quad (4)$$

where  $\mathbf{u}^{(k)}$  and  $m^{(k)}$  are the fluctuating velocity and mass of the  $k$ th particle in the cell, and  $N$  is the number of particles in the cell. Due to statistical and truncation errors, the ensemble mean  $\tilde{\mathbf{u}}$

is not zero exactly. A velocity correction is needed to enforce the consistency condition, e.g.,

$$\mathbf{u}^{(k)} = \mathbf{u}^{(k)*} - \tilde{\mathbf{u}}^*, \tag{5}$$

where the star denotes the uncorrected velocity. In the above correction, the ensemble mean  $\tilde{\mathbf{u}}^*$ , which is random due to the finite number of particles, provides an estimate of the expectation of  $\tilde{\mathbf{u}}^*$ . The ensemble mean of Equation (5) yields

$$\tilde{\mathbf{u}} = \tilde{\mathbf{u}}^* - \tilde{\mathbf{u}}^* = 0, \tag{6}$$

showing that this velocity correction makes  $\tilde{\mathbf{u}}$  identically zero.

Alternatively, the time-averaged ensemble mean of the particle fluctuating velocity, denoted as  $\tilde{\mathbf{u}}^*_{TA}$ , provides a better estimate of the expectation of  $\tilde{\mathbf{u}}^*$ , and the following correction algorithm can be used [15]

$$\mathbf{u}^{(k)} = \mathbf{u}^{(k)*} - \tilde{\mathbf{u}}^*_{TA}. \tag{7}$$

For this correction, we obtain

$$\tilde{\mathbf{u}} = \tilde{\mathbf{u}}^* - \tilde{\mathbf{u}}^*_{TA}, \tag{8}$$

and

$$\langle \tilde{\mathbf{u}} \rangle = 0, \tag{9}$$

since, in the statistically-stationary state considered, we have  $\langle \tilde{\mathbf{u}}^* \rangle = \langle \tilde{\mathbf{u}}^*_{TA} \rangle$ . Thus, for this correction, and for non-trivial time averaging (i.e.,  $N_{TA} > 1$ ),  $\tilde{\mathbf{u}}$  is not identically zero, but it has zero expectation.

To understand the above two correction algorithms (Equations (5) and (7)), we consider the influence of the corrections on the variance of the fluctuating velocity  $\text{var}(u_i)$ . For simplicity we perform the analysis for a single component of velocity, which we denote by  $u$ . In the limit of  $N_{TA} \rightarrow \infty$ ,  $\tilde{u}^*_{TA}$  tends to  $\langle u^* \rangle$ , and it immediately follows from Equation (7) that

$$\text{var}(u) = \text{var}(u^*). \tag{10}$$

Hence, the correction (Equation (7)) is unbiased in the sense that the variances of fluctuating velocity evaluated before and after the correction are the same as  $N_{TA} \rightarrow \infty$ .

The correction Equation (5) yields

$$\text{var}(u) = \text{var}(u^*) + \text{var}(\tilde{u}^*) - 2\text{cov}(u^*, \tilde{u}^*), \tag{11}$$

where  $\text{cov}(\ )$  denotes covariance. If we assume that the particles in a cell are statistically identical with equal mass  $m^{(k)}$ , and that the velocities associated with different particles are uncorrelated, it can be verified that

$$\text{var}(\tilde{u}^*) = \frac{1}{N_{pc}} \text{var}(u^*), \tag{12}$$

$$\text{cov}(u^*, \tilde{u}^*) = \frac{1}{N_{pc}} \text{var}(u^*). \tag{13}$$

Thus Equation (11) becomes

$$\text{var}(u) = \left(1 - \frac{1}{N_{\text{pc}}}\right) \text{var}(u^*), \quad (14)$$

showing that the correction Equation (5) is biased in the sense that, for finite  $N_{\text{pc}}$ , it decreases the variance of the fluctuating velocity.

Now we turn our attention to the expectations of the turbulent kinetic energy (TKE)  $k^*$  and  $k$  evaluated before and after the velocity correction, respectively,

$$\begin{aligned} \langle k^* \rangle &= \frac{1}{2} \langle \widetilde{u_i^* u_i^*} \rangle = \frac{1}{2} (\langle \widetilde{u_i^* u_i^*} \rangle - \langle \widetilde{u_i^*} \rangle \langle \widetilde{u_i^*} \rangle) + \frac{1}{2} \langle \widetilde{u_i^*} \rangle \langle \widetilde{u_i^*} \rangle \\ &= \frac{1}{2} \sum_{i=1}^3 \text{var}(u_i^*) + \frac{1}{2} \langle \widetilde{u_i^*} \rangle \langle \widetilde{u_i^*} \rangle, \end{aligned} \quad (15)$$

$$\begin{aligned} \langle k \rangle &= \frac{1}{2} \langle \widetilde{u_i u_i} \rangle = \frac{1}{2} (\langle \widetilde{u_i u_i} \rangle - \langle \widetilde{u_i} \rangle \langle \widetilde{u_i} \rangle) + \frac{1}{2} \langle \widetilde{u_i} \rangle \langle \widetilde{u_i} \rangle \\ &= \frac{1}{2} \sum_{i=1}^3 \text{var}(u_i) + \frac{1}{2} \langle \widetilde{u_i} \rangle \langle \widetilde{u_i} \rangle. \end{aligned} \quad (16)$$

The underlying assumption involved in the above equations are that all the particles in the same cell are statistically identical so the variance of fluctuating velocity of each particle is the same. In the above analysis, we observe that both corrections (Equations (5) and (7)) yield  $\langle \widetilde{u_i} \rangle = 0$ , so from Equations (15) and (16), we have

$$\langle k \rangle - \langle k^* \rangle = \frac{1}{2} \sum_{i=1}^3 [\text{var}(u_i) - \text{var}(u_i^*)] - \frac{1}{2} \langle \widetilde{u_i^*} \rangle \langle \widetilde{u_i^*} \rangle. \quad (17)$$

For correction Equation (7), the first term on the right-hand side of the above equation disappears due to Equation (10), so Equation (17) reduces to

$$\langle k \rangle - \langle k^* \rangle = -\frac{1}{2} \langle \widetilde{u_i^*} \rangle \langle \widetilde{u_i^*} \rangle. \quad (18)$$

It can be seen that the correction Equation (7) removes the mean kinetic energy contained in the TKE evaluated before the correction. For finite  $N_{\text{TA}}$  the analysis is more involved, but the bias shown in Equation (18) is likely to remain, albeit of a small magnitude.

For the correction Equation (5), however, the first term on the right-hand side of Equation (17) does not disappear, and by substituting Equation (14) into Equation (17), we have

$$\langle k \rangle - \langle k^* \rangle = -\frac{1}{2N_{\text{pc}}} \sum_{i=1}^3 \text{var}(u_i^*) - \frac{1}{2} \langle \widetilde{u_i^*} \rangle \langle \widetilde{u_i^*} \rangle. \quad (19)$$

For each time step  $\Delta t$ , the correction Equation (5) corresponds to a fractional step for the variation of TKE, i.e.,

$$\left\langle \frac{dk}{dt} \right\rangle_{\text{correction}} = \frac{\langle k \rangle - \langle k^* \rangle}{\Delta t} = -\varepsilon_n - \frac{\langle \tilde{u}_i^* \rangle \langle \tilde{u}_i^* \rangle}{2\Delta t}, \quad (20)$$

where  $\varepsilon_n = \frac{1}{2N_{pc}\Delta t} \sum_{i=1}^3 \text{var}(u_i^*) > 0$ . In addition to removing the mean kinetic energy contained in the TKE evaluated before the correction, the correction Equation (5) introduces a numerical dissipation  $\varepsilon_n$  which reduces the TKE. As  $N_{pc}$  tends to infinity,  $\varepsilon_n$  tends to zero, so the two corrections (Equations (5) and (7)) are consistent in this limit. If the physical dissipation  $\varepsilon$  and the numerical dissipation  $\varepsilon_n$  are linearly related, the total dissipation rate of TKE  $\varepsilon_{\text{tot}}$  in the computation is the sum of them

$$\varepsilon_{\text{tot}} = \varepsilon + \varepsilon_n. \quad (21)$$

To summarize, the correction Equation (7) produces zero expectation of the fluctuating velocity and conserves its variance, and removes the mean kinetic energy from the TKE evaluated before the correction. Although the correction Equation (5) produces identically zero ensemble mean of the fluctuating velocity, it reduces the variance of the velocity. As a consequence, it introduces a numerical dissipation term in the TKE evolution, in addition to removing the mean kinetic energy contained in the TKE evaluated before the correction.

### 3. Influence of time-averaging on bias

To quantify the influence of the time-averaging of mean fluctuating velocity on bias, two test cases, the Cabra  $\text{H}_2/\text{N}_2$  lifted flame [19] and the Sandia piloted flame E [20], are performed and described in the following subsections.

#### 3.1. Cabra lifted $\text{H}_2/\text{N}_2$ jet flame

The Cabra lifted  $\text{H}_2/\text{N}_2$  jet flame has been investigated using the hybrid FV/particle PDF method in [7]. The details of the current simulation are the same as those in [7], i.e., the  $\text{H}_2/\text{O}_2$  reaction mechanism (the Li mechanism or the Mueller mechanism used in [7]), the EMST model ( $C_\phi = 1.5$ ), the simplified Langevin model, the stochastic frequency model with  $C_{\omega 1} = 0.65$ , the calculated inlet velocity profiles, the number of particles per cell  $N_{pc} = 100$ . Any differences in the details of the simulation from [7] are mentioned below.

The test cases shown below use the same models and parameters (EMST, Li mechanism, coflow temperature  $T_c = 1033$  K) as those used in Figure 16 of [7], except for the values of  $C_\phi$ ,  $N_{pc}$ , and the time-averaging of the mean fluctuating velocity. The value of  $C_\phi$  used here is 1.5 rather than 2.0 in Figure 16 of [7]. The influence of  $C_\phi$  on the results with  $T_c = 1033$  K is negligible (see Figure 8 in [7]). The value of  $N_{pc}$  varies from 100 to 250 in these test cases. For each value of  $N_{pc}$ , two cases are compared, one case with all quantities time-averaged (denoted as TAU), and the other with all quantities except the mean fluctuating velocity time-averaged (denoted as NoTAU). Figure 1 shows the mean axial velocity  $\tilde{U}$ , the mean turbulence frequency  $\tilde{\omega}$ , the Reynolds stresses  $\tilde{u}u$ ,  $\tilde{u}v$ , and the means and rms of the mixture fraction and temperature plotted against  $N_{pc}^{-1}$  at the location  $(x, r) = (15D, 1D)$  in the Cabra lifted  $\text{H}_2/\text{N}_2$  jet flame, where  $(x, r)$  are the axial and radial coordinates, and  $D$  is the diameter of the fuel jet nozzle. Several observations can be made from the figure. First, the results by the two methods (TAU and

NoTAu) vary linearly with  $N_{pc}^{-1}$ , reflecting the expected scaling of the bias [12, 18]. Second, when extrapolated to  $N_{pc} \rightarrow \infty$  (i.e.,  $N_{pc}^{-1} = 0$ ) the two methods (TAu and NoTAu) yield almost the same results, indicating the convergence of both methods to the same solution. Third, the slopes of the results obtained with TAu are much smaller in magnitude than those obtained by NoTAu, implying that TAu reduces the bias in the hybrid algorithm dramatically compared to the NoTAu case. Fourth, with TAu, all the results obtained with different values of  $N_{pc}$  (from 100 to 250) fall inside the  $\pm 5\%$  error lines, so the value of  $N_{pc} = 100$  used in [7] is a reasonable choice for the simulations. Last, with NoTAu,  $\langle uu \rangle$  decreases with increasing  $N_{pc}^{-1}$ , consistent with the argument related to numerical dissipation  $\varepsilon_n$  (Equation 20). However, this is generally true for upstream locations, e.g.,  $x \leq 35D$ . At downstream locations,  $\langle uu \rangle$  may increase with increasing  $N_{pc}^{-1}$ . Comparing the results reported in [7] with the current results, we confirm that the presented results with TAu and  $N_{pc} = 100$  are consistent with those in [7].

Figure 1 demonstrates that TAu has a substantial effect on the bias involved in unconditional statistics. The influence of TAu on conditional means is now investigated. In Figure 2 are shown the conditional means of temperature, mass fractions of  $H_2O$  and  $OH$  against  $N_{pc}^{-1}$  at  $x/D = 15$  and  $26$  in the Cabra  $H_2/N_2$  lifted jet flame, where the means are conditional on the mixture fraction  $\xi$  being in the ranges  $[\xi_l, \xi_u]$  indicated in the figure. The ranges of mixture fraction are particularly chosen to cover the peaks where most sensitivity is expected. In contrast to the

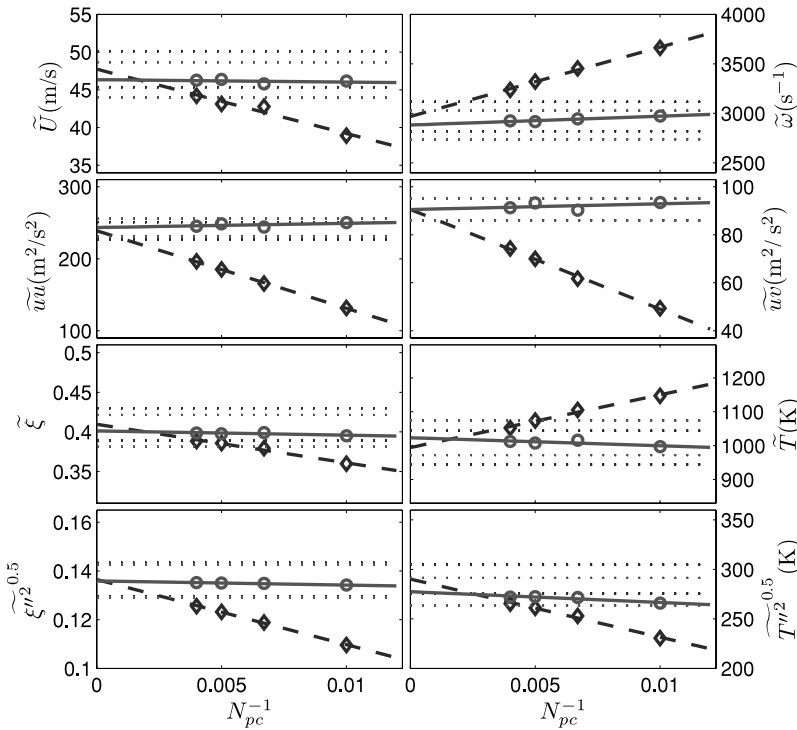


Figure 1. PDF calculations of the means of the axial velocity  $\tilde{U}$ , the turbulence frequency  $\tilde{\omega}$ , the Reynolds stress  $\tilde{uu}$ ,  $\tilde{uv}$ , and the means and rms of the mixture fraction and temperature against  $N_{pc}^{-1}$  at the location of  $(15D, 1D)$  in the Cabra lifted  $H_2/N_2$  jet flame. (Circle: TAu; Diamond: NoTAu; Solid or dashed lines: linear least square fit; Dotted lines:  $\pm 5\%$  error.)

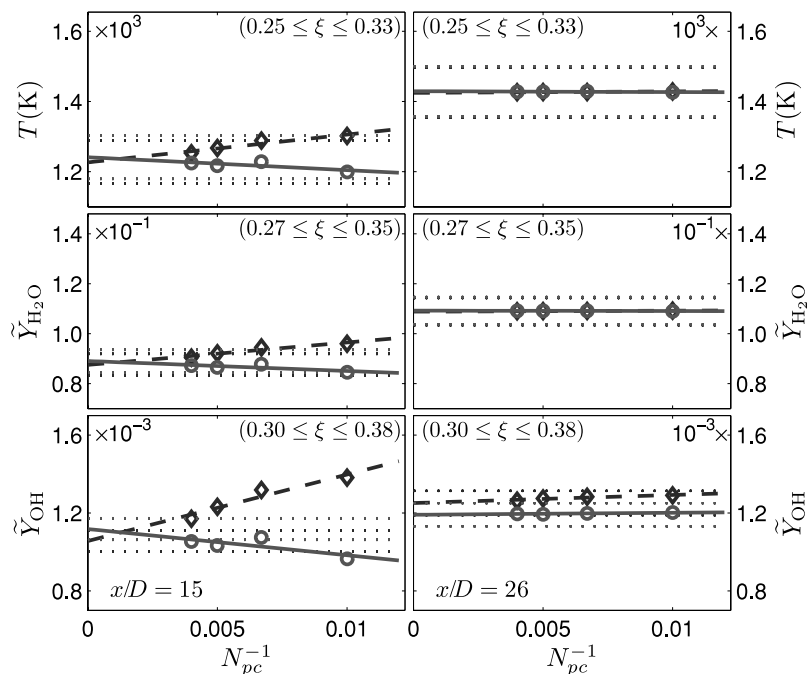


Figure 2. The conditional means of the temperature and mass fractions of  $\text{H}_2\text{O}$  and  $\text{OH}$  against  $N_{pc}^{-1}$  at the location of  $x/D = 15$  (left) and  $26$  (right) in the Cabra lifted  $\text{H}_2/\text{N}_2$  jet flame. (Circle: TAu; Diamond: NoTAu; Solid or dashed lines: linear least square fit; Dotted lines:  $\pm 5\%$  error.)

unconditional statistics in Figure 1, the bias involved in the calculations of conditional means obtained with NoTAu (Figure 2) is small. The results at  $x/D = 15$  exhibit a larger sensitivity because this location is close to the base of the flame. In summary, the conditional statistics are affected little by the time-averaging strategy, which is very different from the case of the unconditional statistics.

### 3.2. Sandia piloted flame E

The simulation results of flame E obtained using HYB2D are reported recently in [5, 6]. If not specially mentioned, the details of the current simulation are the same as in [5, 6]. The test cases here use the EMST model with  $C_\phi = 1.5$ , the skeletal mechanism [21], the value  $C_{\omega 1} = 0.65$  and ignore radiation. Figure 3 shows the means of the axial velocity  $\bar{U}$ , turbulence frequency  $\tilde{\omega}$ , the Reynolds stress  $\tilde{uu}$ ,  $\tilde{uv}$ , and the means and rms of the mixture fraction and temperature against  $N_{pc}^{-1}$  at the location of  $(45D, 1D)$ . Similar observations to the case of the Cabra lifted flame can be made. The Reynolds stress  $\langle uu \rangle$ , however, increases with  $N_{pc}^{-1}$  at the axial location shown. At upstream locations (e.g.,  $x \leq 40$ ),  $\langle uu \rangle$  decreases with  $N_{pc}^{-1}$  generally. Figure 4 shows the conditional means of the temperature and mass fractions of  $\text{CO}_2$ ,  $\text{H}_2\text{O}$ ,  $\text{CO}$ ,  $\text{H}_2$  and  $\text{OH}$  against  $N_{pc}^{-1}$  at the location of  $x/D = 45$ . The bias involved in the conditional statistics in flame E obtained using TAu and NoTAu is very small (below 5%).

In the above discussion of both test cases, results are shown only at a few locations, but they are representative of all other locations of interest, i.e., two or three diameters downstream from

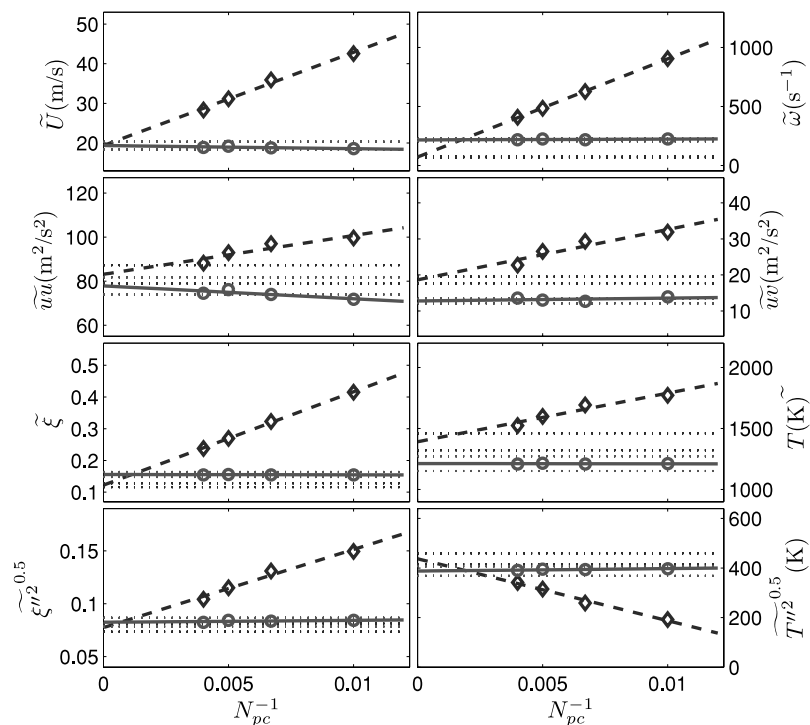


Figure 3. PDF calculations of the means of the axial velocity  $\tilde{U}$ , turbulence frequency  $\tilde{\omega}$ , the Reynolds stress  $\tilde{uu}$ ,  $\tilde{uv}$ , and the means and rms of the mixture fraction and temperature against  $N_{pc}^{-1}$  at the location of  $(45D, 1D)$  in the Sandia piloted flame E. (Circle: TAU; Diamond: NoTAU; Solid or dashed lines: linear least square fit; Dotted lines:  $\pm 5\%$  error.)

the nozzle. The results near the nozzle are very sensitive to the imposed inlet boundary condition, so they are not appropriate for the current discussion.

### 3.3. Discussion

Based on the test cases of the Cabra lifted  $H_2/N_2$  flame and the Sandia flame E by using TAU and NoTAU, it can be concluded that both TAU and NoTAU are legitimate, consistent methods in the sense that they converge to the same results as  $N_{pc}$  tends to infinity. For finite  $N_{pc}$  (e.g., 100), TAU reduces the bias involved in unconditional statistics of PDF calculations considerably. It confirms the correct design of the original velocity correction algorithm (Equation 7) [15]. The results of the Cabra lifted  $H_2/N_2$  flame reported in [7] are reproduced by using the current version of the HYB2D with TAU. Compared to the early versions of the HYB2D used in [5–7], several minor corrections and modifications have been made, and a new version of the ISAT library [22] is used. The influence of these changes has been evaluated carefully and are found to be negligible. The current bias convergence tests and the consistency of the Cabra lifted flame results with the early version and the current updated version of the HYB2D enhance our confidence in the correctness of the implementation of the PDF method. The current results of flame E with NoTAU and  $N_{pc} = 100$  are consistent with those reported in [5, 6]. Thus, large bias is involved in the unconditional statistics reported in [5, 6] due to the disabled time-averaging of the

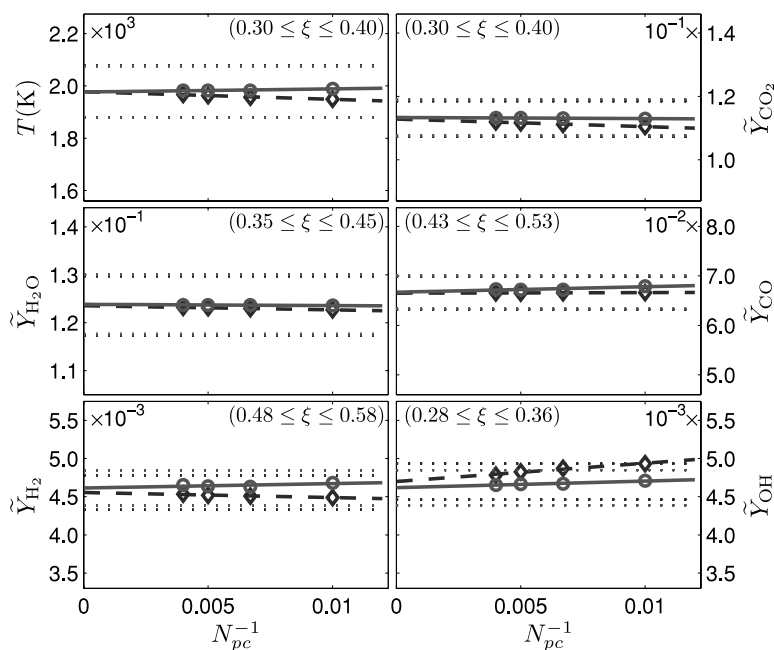


Figure 4. The conditional means of the temperature and mass fractions of  $\text{CO}_2$ ,  $\text{H}_2\text{O}$ ,  $\text{CO}$ ,  $\text{H}_2$  and  $\text{OH}$  against  $N_{pc}^{-1}$  at the location of  $x/D = 45$  in the Sandia piloted flame E. (Circle: TAu; Diamond: NoTAu; Solid or dashed lines: linear least square fit; Dotted lines:  $\pm 5\%$  error.)

particle-to-particle quantities. However, this bias does not affect the conclusions drawn in those papers. First, the inaccuracy of the results do not affect the qualitative conclusions of the relative performance of different reaction mechanisms drawn in [6] and of the relative performance of different mixing models drawn in [5]. Second, TAu affects the velocity field and the mixing field directly. Once the velocity field and the mixing field are somehow calculated reasonably compared to the experimental data as in [5, 6], the mixing process and the chemical reaction process are not expected to be altered dramatically no matter the time-averaging strategy, as indicated by the conditional statistics in Figures 2 and 4. This is discussed further in the next section.

#### 4. Influence of the model constant $C_{\omega 1}$

We have seen that bias, to some extent, corresponds to additional dissipation of TKE. In the stochastic turbulence frequency model [8], increasing the model constant  $C_{\omega 1}$  also leads to increased dissipation rate of TKE. In the numerical simulation, it is the total dissipation rate (physical plus numerical, Equation 21) which affects the TKE. Hypothetically, a decrease in  $C_{\omega 1}$  can compensate for the bias error. This is an important issue for the following reason. The studies of these flames (e.g., the Cabra flame and flame E) over the past decade have focused on the details of the turbulence-chemistry interactions. In order to minimize the effects of shortcomings in the turbulence models, the general practice is to adjust  $C_{\omega 1}$  (or  $C_{\varepsilon 1}$ ) as needed to achieve the observed jet spreading rates (as revealed by the radial profiles of mean mixture fraction, for example), and different values for  $C_{\omega 1}$  have been used, e.g., 0.56 in [3], and 0.65 in [5–7]. According to the

above hypothesis, calculations involving substantial bias require lower values of  $C_{\omega_1}$  (compared to bias-free calculations) in order to match the observed jet spreading rates.

To test this hypothesis, PDF calculations with TAU or NoTAU (involving different amounts of bias) and with different values of  $C_{\omega_1}$  are performed for the Cabra lifted flame and for Sandia flame E. Figures 5 and 6 show the radial profiles of the means and rms of the mixture fraction, temperature and OH mass fraction at different axial locations in the Cabra lifted  $H_2/N_2$  jet flame and in the Sandia flame E. The same numerical settings as in Figure 1 are used with  $N_{pc} = 100$ ,  $C_{\omega_1} = 0.56$  or  $0.65$ , and TAU or NoTAU for the Cabra flame. For the results with the different values of  $C_{\omega_1}$  using NoTAU in Figure 5, we can see that increasing  $C_{\omega_1}$  decreases the jet spreading rate and rms of the mixture fraction, so we confirm that the higher the value of  $C_{\omega_1}$ , the more dissipative is the turbulence model. For the same value of  $C_{\omega_1} (= 0.65)$ , NoTAU gives an under-prediction of the jet spreading rate and of the rms mixture fraction because of the numerical dissipation  $\varepsilon_n$  involved in NoTAU which weakens the turbulent transport. Comparing the results with TAU and  $C_{\omega_1} = 0.65$  and the results with NoTAU and  $C_{\omega_1} = 0.56$  in Figure 5, we can see that both cases give very similar predictions of the radial mean and rms profiles of the mixture fraction, temperature, and OH mass fraction.

For flame E in Figure 6, the numerical settings are the same as in Figure 3 with  $N_{pc} = 100$ , TAU or NoTAU, and different values for  $C_{\omega_1}$ . The results with NoTAU and  $C_{\omega_1} = 0.65$  (solid lines

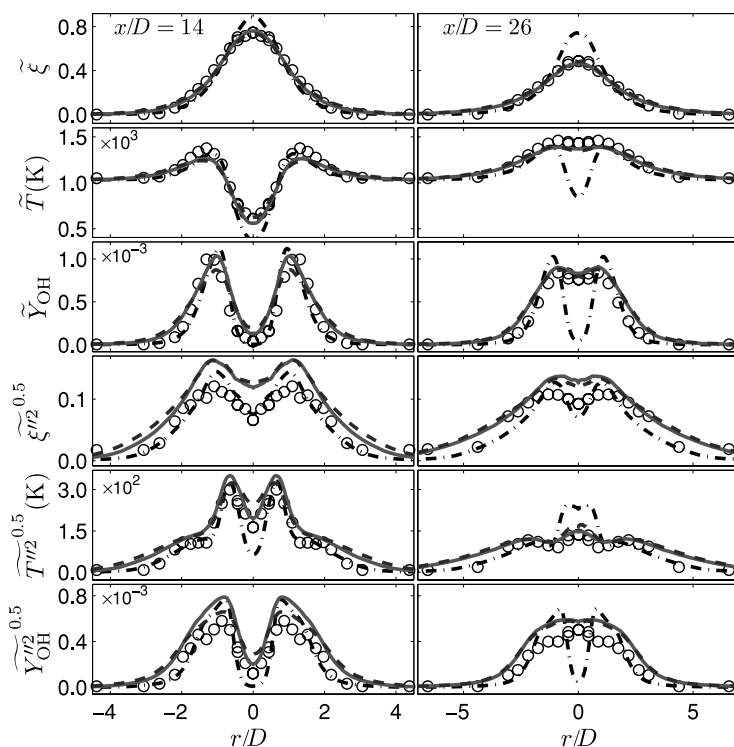


Figure 5. Radial profiles of the means and rms of the mixture fraction, temperature and OH mass fraction at the axial locations of  $x/D = 14$  and  $26$  in the Cabra lifted  $H_2/N_2$  jet flame. (Circles: experimental data; Curves: PDF calculations using TAU with  $C_{\omega_1} = 0.65$  (solid), using NoTAU with  $C_{\omega_1} = 0.56$  (dashed), and using NoTAU with  $C_{\omega_1} = 0.65$  (dash-dotted).)

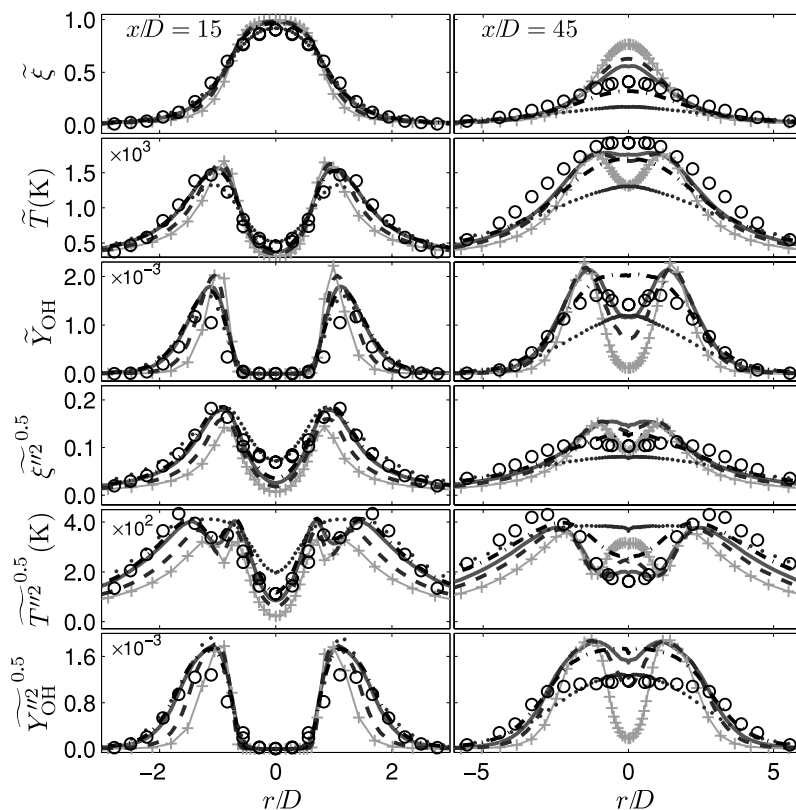


Figure 6. Radial profiles of the means and rms of the mixture fraction, temperature and OH mass fraction at the axial locations of  $x/D = 15$  and  $45$  in the Sandia flame E. (Circles: experimental data; Curves: PDF calculations using NoTAU with  $C_{\omega 1} = 0.65$  (solid line), using TAU with  $C_{\omega 1} = 0.85$  (solid line with plus), using TAU with  $C_{\omega 1} = 0.75$  (dashed line), using TAU with  $C_{\omega 1} = 0.70$  (dash-dotted line), and using TAU with  $C_{\omega 1} = 0.65$  (dotted line).)

in Figure 6) agree with the experimental data very well (equivalent to the results presented in [5, 6]), even though considerable bias is involved in the results. If TAU is used with  $C_{\omega 1} = 0.65$  (dotted lines in Figure 6), the jet spreading rate is over-predicted as expected (because numerical dissipation is removed by TAU). To achieve the same jet spreading rate using TAU as using NoTAU with  $C_{\omega 1} = 0.65$ , it is necessary to increase  $C_{\omega 1}$ . The results with different values of  $C_{\omega 1}$  ( $= 0.70$  (dash-dotted lines),  $0.75$  (dashed lines), and  $0.85$  (solid lines with plus)) for flame E are compared in Figure 6. To match the mean and rms profiles of the mixture fraction with the experimental data, we can see that  $C_{\omega 1} = 0.70$  is a reasonable choice. The results by TAU and  $C_{\omega 1} = 0.70$  (dashed line) and by NoTAU and  $C_{\omega 1} = 0.65$  (points) in Figure 6 are still different, but their overall agreement with the experimental data is similar. Thus, in some sense, the effect of the bias error in the PDF calculations is similar to the effect of increasing the value of  $C_{\omega 1}$ .

In the previous PDF calculations, different values for  $C_{\omega 1}$  are used, e.g.,  $0.56$  in [3], and  $0.65$  in [5–7]. In the calculations of the Sandia piloted flames by using the stand-alone particle method [3], the good agreement between the numerical results and the experimental data is achieved by using  $C_{\omega 1} = 0.56$ . The stand-alone particle method is expected to involve bias [18]. In the

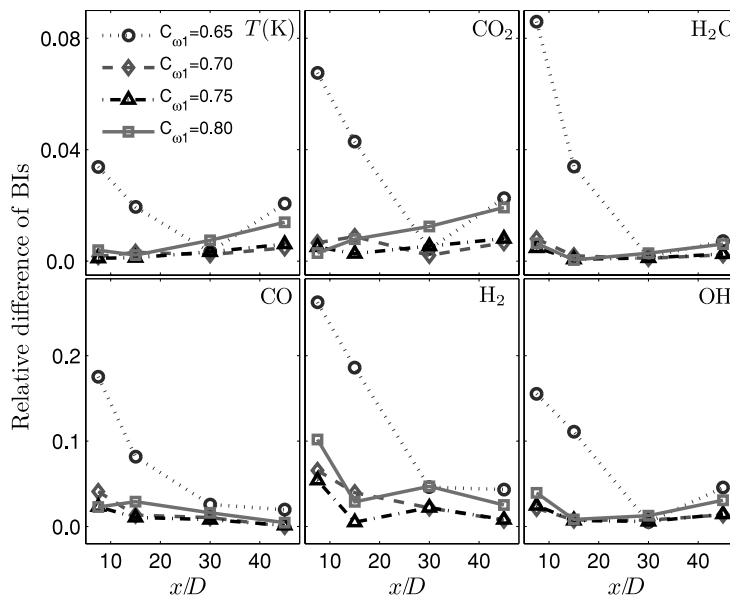


Figure 7. The difference in the BIs by TAU and different values of  $C_{\omega_1}$  relative to the BI by NoTAU and  $C_{\omega_1} = 0.65$ .

later calculations of the same flames by using the hybrid FV/particle method [5, 6], very similar results are obtained by using  $C_{\omega_1} = 0.65$ . The bias in [5, 6] is not small due to the disabled time-averaging. However, the bias involved in the results in [5, 6] should still be less than that in the results in [3] because the smooth FV fields are used in the particle method. By using TAU, we use a higher value  $C_{\omega_1} = 0.7$  by using the hybrid method to produce the similar results to those in [5, 6]. Evidently, the increases in the value of  $C_{\omega_1}$  used is a result of the decreasing bias error during the development of the solution algorithm of the PDF method.

The burning index (BI) is often used to quantify the amount of local extinction in the Sandia piloted flames. To evaluate the sensitivity of the BIs to the values of  $C_{\omega_1}$  and to the time-averaging, the relative difference of the BIs are presented in Figure 7 by TAU and different values of  $C_{\omega_1}$  relative to the BIs by NoTAU and  $C_{\omega_1} = 0.65$  (equivalent to the results in [5, 6]). The BIs are calculated in the identical way to those in [3, 6]. The relative difference of BIs based on the temperature and the species mass fractions with  $C_{\omega_1} = 0.65$  is evident (up to 25% for  $H_2$  mass fraction at  $x/D = 7.5$ ). The relative difference of BIs with  $C_{\omega_1} > 0.65$  for all the test cases is within 5% except for  $H_2$  mass fraction at  $x/D = 7.5$  whose relative difference is within 11%. The small relative difference of the current updated results by using different values of  $C_{\omega_1}$  ( $> 0.65$ ) and TAU relative to the results presented in [5, 6] for flame E demonstrates that the qualitative conclusions drawn in [5, 6] are not affected by the bias involved in those results.

The results presented in [3, 5, 6] and in this paper are quite similar, all in good agreement with the experimental data. This reminds us that good agreement between numerical results and experimental data does not necessarily indicate the numerical accuracy of numerical methods. The numerical errors can be compensated for somehow by adjusting model constants. A comprehensive exploration of numerical properties (such as numerical accuracy and convergence) of numerical methods is crucial for today's numerical simulations.

## 5. Conclusion

The time-averaging strategies in the hybrid solution method of the joint PDF method are investigated. The time-averaging of the mean fluctuating velocity (TAu) leads to the same variances of the fluctuating velocity before and after the velocity correction for a fixed number of particles per cell over a long time-averaging scale. Without TAu, the variances of the fluctuating velocity before and after the velocity correction are different, and an additional numerical dissipation is introduced for the turbulent kinetic energy. TAu reduces dramatically the bias involved in the unconditional statistics of the tested turbulent flames, the Cabra  $\text{H}_2/\text{N}_2$  lifted flame and the Sandia flame E. The conditional statistics in these flame, however, are hardly affected by TAu. The effect of the bias involved in the unconditional statistics is similar to the effect of increasing the value of the model constant  $C_{\omega 1}$ . The value of 0.7 for  $C_{\omega 1}$  is suggested to yield the similar results of flame E with TAu to those without TAu and with 0.65 in [6, 5] (also in good agreement with the experimental data).

## Acknowledgements

This work is supported by the Air Force Office of Scientific Research, Grant FA9550-06-1-0048. We are grateful to Steven R. Lantz and Daniel I. Sverdluk for their help on the parallel computations, and to Renfeng Cao for help on the HYB2D code. Various suggestions from David A. Caughey and Zhuyin Ren are appreciated. This research was conducted using the resources of the Cornell Theory Center, which receives funding from Cornell University, New York State, federal agencies, foundations, and corporate partners.

## References

- [1] S.B. Pope, *PDF methods for turbulent reactive flows*, Prog. Energy Combust. Sci. 11 (1985), pp. 119–192.
- [2] S.B. Pope, *Turbulent Flows*, Cambridge University Press, Cambridge, 2000.
- [3] J. Xu and S.B. Pope, *PDF calculations of turbulent nonpremixed flames with local extinction*. Combust. Flame 123 (2000), pp. 281–307.
- [4] R.P. Lindstedt, S.A. Louloudi, and E.M. Vaos, *Joint scalar probability density function modeling of pollutant formation in piloted turbulent jet diffusion flames with comprehensive chemistry*, Proc. Combust. Inst. 28 (2000), pp. 149–156.
- [5] R.R. Cao, H. Wang, and S.B. Pope, *The effect of mixing models in PDF calculations of piloted jet flames*, Proc. Combust. Inst. 31 (2007), pp. 1543–1550.
- [6] R.R. Cao and S.B. Pope, *The influence of chemical mechanisms on PDF calculations of nonpremixed piloted jet flames*, Combust. Flame 143 (2005), pp. 450–470.
- [7] R.R. Cao, S.B. Pope, and A.R. Masri, *Turbulent lifted flames in a vitiated coflow investigated using joint PDF calculations*, Combust. Flame 142 (2005), pp. 438–453.
- [8] P.R. Van Slooten, Jayesh, and S.B. Pope, *Advances in PDF modeling for inhomogeneous turbulent flows*, Phys. Fluids 10 (1998), pp. 246–265.
- [9] S.B. Pope, *A stochastic Lagrangian model for acceleration in turbulent flows*, Phys. Fluids 14 (2002), pp. 2360–2375.
- [10] S. Subramaniam and S.B. Pope, *A mixing model for turbulent reactive flows based on Euclidean minimum spanning trees*, Combust. Flame 115 (1998), pp. 487–514.
- [11] S.B. Pope, *A Monte Carlo method for the PDF equations of turbulent reactive flow*, Combust. Sci. Technol. 25 (1981), pp. 159–174.
- [12] S.B. Pope, *Particle method for turbulent flows: integration of stochastic model equations*, J. Comput. Phys. 117 (1995), pp. 332–349.
- [13] M. Muradoglu, P. Jenny, S.B. Pope, and D.A. Caughey, *A consistent hybrid finite-volume/particle method for the PDF equations of turbulent reactive flows*, J. Comput. Phys. 154 (1999), pp. 342–371.
- [14] P. Jenny, S.B. Pope, M. Muradoglu, and D.A. Caughey, *A hybrid algorithm for the joint PDF equation for turbulent reactive flows*, J. Comput. Phys. 166 (2001), pp. 218–252.
- [15] M. Muradoglu, S.B. Pope, and D.A. Caughey, *The hybrid method for the PDF equations of turbulent reactive flows: consistency conditions and correction algorithms*, J. Comput. Phys. 172 (2001), pp.

- 841–878.
- [16] Y.Z. Zhang and D.C. Haworth, *A general mass consistency algorithm for hybrid particle/finite-volume PDF methods*, J. Comput. Phys. 194 (2004), pp. 156–193.
  - [17] K. Liu, *Joint velocity-turbulence frequency-composition probability density function (PDF) calculations of bluff body stabilized flames*, Ph.D. diss., Cornell University, 2004.
  - [18] J. Xu and S.B. Pope, *Assessment of numerical accuracy of PDF/Monte Carlo methods for turbulent reactive flows*, J. Comput. Phys. 152 (1999), pp. 192–230.
  - [19] R. Cabra, T. Myhrvold, J.-Y. Chen, *et al.*, *Simultaneous laser Raman-Rayleigh-LIF measurements and numerical modeling results of a lifted turbulent  $H_2/N_2$  jet flame in a vitiated coflow*, Proc. Combust. Inst. 29 (2002), pp. 1881–1888.
  - [20] R.S. Barlow and J.H. Frank, *Effects of turbulence on species mass fractions in methane–air jet flames*, Proc. Combust. Inst. 27 (1998), pp. 1087–1095.
  - [21] S. James, M.S. Anand, M.K. Razdan, and S.B. Pope, *In situ detailed chemistry calculations in combustor flow analysis*. ASME J. Engng. Gas Turbines Power 123 (2001), pp. 747–756.
  - [22] S.B. Pope, *Computationally efficient implementation of combustion chemistry using in situ adaptive tabulation*, Combust. Theory Model. 1 (1997), pp. 41–63.
  - [23] M. Muradoglu, K. Liu, and S.B. Pope, *PDF modeling of a bluff-body stabilized turbulent flame*, Combust. Flame 132 (2003), pp. 115–137.